PHYSICAL REVIEW B VOLUME 22, NUMBER 10 15 NOVEMBER 1980

Electronic structure of the Tl^+ center in KCl. II. Relation to the D band

Taiju Tsuboi
Department of Physics, Kyoto Sangyo University, Kamigamo, Kyoto 603, Japan

Shoichiro Sakoda
Division of Junior College, Osaka Electro-Communication University, Neyagawa, Osaka 572, Japan

(Received 15 April 1980)

It has been shown that the D band in alkali halides containing s^2 ion (Tl^+, In^+, Ga^+, Sn^{2+}) is composed of three bands (named D_1, D_2, D_3 in the order of increasing energy). Of the three bands, the D_1 band is the weakest whereas the D_2 band is the strongest. In KCl:Tl^+, the D_1 band is observed at about 6.72 eV whereas the D_2 band is observed at about 7.23 eV. A theoretical calculation using molecular orbitals has been made on the charge-transfer-type transition $(e_g)^4 \rightarrow (e_g)^3(t_{1u}^*)$ in a $(TlCl_6)^{5-}$ complex to clarify the origin of the D band in KCl:Tl^+. The configuration interaction with $(a_{1g}^*)(t_{1u}^*)$ configuration responsible for the A, B, and C bands is taken into account in the calculation. Three absorption bands are theoretically derived; one is located at 7.74 eV, the others at 7.28 and 6.71 eV. It is shown that the latter two bands correspond well to the observed D_2 and D_1 bands, respectively. It is also demonstrated that the theoretically derived 7.74-eV band is not observed experimentally being hidden under the much stronger exciton band. The present calculation also gives a satisfactory agreement with experiment for the A and C band positions.

I. INTRODUCTION

In addition to the A, B, and C bands, an absorption band called D band has been observed in the spectral region between the C band and exciton band in various alkali halides doped with s^2 ions (Tl^+, In^+, Ga^+, Sn^{2+}, and Pb^{2+}).[1-12] It is well established that the A, B, and C bands arise from electronic transition associated with $s^2 \rightarrow sp$ transition in the s^2 ions, while the accurate origin of the D band is unknown. So far, two distinct assignments have been suggested for the D band. One assignment is that the D band arises from the exciton perturbed by the presence of the s^2 ion, namely, electron transfer from a halide ion to an alkali ion in the vicinity of s^2 ion (Refs. 3 and 4) (perturbed exciton model), and the other is that the D band arises from electron transfer from ligand halide ions to central s^2 ion in a MX_6 (M, s^2 ion; X, halide ion) quasimolecule[10-14] (charge-transfer model). The charge-transfer model seems to be more reasonable, but it has not been established quantitatively from a theoretical point of view.

The present paper is concerned with the assignment of the D band. This work was originally undertaken in an effort to explain the origins of all the A, B, C, and D bands consistently. Here we first investigate the optical properties of the D band in various s^2-ion–doped alkali halides experimentally, especially on its fine structure, and show the characteristics common to various alkali halides. Next, taking into account the configuration interaction with the A, B, and C bands, we make a calculation on the electronic state responsible for the D band in KCl : Tl^+.

In a previous paper[15] (referred to as I hereafter), we made a molecular orbital (MO) calculation and clarified the electronic states responsible for the A, B, and C bands in KCl : Tl^+ quantitatively. The result of the MO calculation is used in the present work. Although we are here concerned with KCl : Tl^+ (KCl : Tl^+ is the only case for which theoretical calculations have been carried out), characteristics of our theoretically-derived result may be common to various s^2-ion–doped crystals.

II. ABSORPTION SPECTRA OF THE D BAND

The absorption spectra shown in this paper were taken using a Shimadzu spectrophotometer MPS-50L and a McPherson 0.3-meter scanning monochromator Model 218 for the measurements of ultraviolet and vacuum ultraviolet regions, respectively. Single crystals of s^2-ion–doped alkali halides were grown by the Kyropoulos method, whereas single crystals of undoped KI and KCl by the Harshaw Chemical Company.

Three components called D_1, D_2, and D_3 bands are observed in the D band of KI : Sn^{2+} at 15 K as seen in Fig. 1.[11] These components are close to each other, and, at a high temperature such as 77 K, the D_1 and D_2 bands were found but the D_3 band was hidden under the broad exciton band. Figure 2 shows the absorption spectrum of KCl : Sn^{2+} at 77 K, where two components (D_1 and D_2) are observed in the D band. The structure of the D band of KCl : Sn^{2+} is quite similar to that of KI : Sn^{2+} which was taken at the same 77 K.

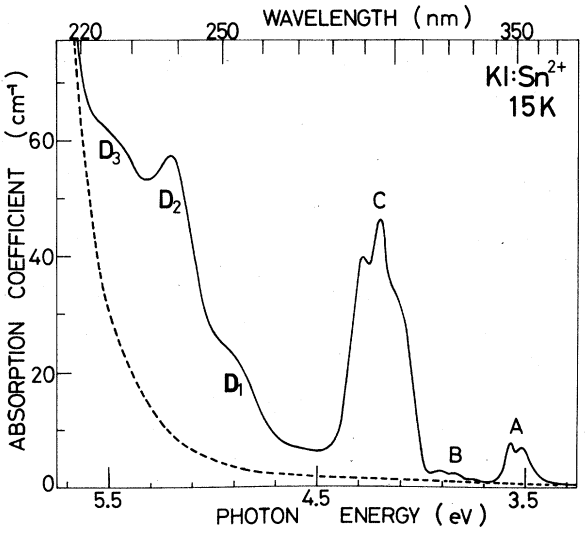

FIG. 1. Absorption spectra of a $KI:Sn^{2+}$ (0.005 mole % in the melt, solid line) and an undoped KI (dashed line) crystals at 15 K.

Figure 3 shows the absorption spectrum of $KI:Tl^+$ at 15 K. The well-known D band[1,4] is observed to have a peak at 5.537 eV (223.9 nm), which is named as D_2 in Fig. 3 tentatively. At a low temperature, such as 15 K, a weak shoulder is found at 5.600 eV (221.4 nm) on the high energy side of the D_2 band, which is called D_3. A similar shoulder has been observed in $KI:In^+$ and $KI:Ga^+$ by their excitation spectra.[7] We tried to find another component of the D band in the spectral region between the C and D_2 bands in $KI:Tl^+$, but it was not clearly observed because, unlike the case of $KI:Sn^{2+}$, the C and D_2 bands are close to each other. It was difficult to estimate the intensity of each of the D_2 and D_3 bands since both bands overlap with each other. The total intensity of both bands was obtained by subtracting the tail of the exciton band, from which the oscillator strength f was estimated to be $f=0.30$.

Figure 4 shows the absorption spectra of $KCl:Tl^+$ and $KCl:In^+$ at 77 K. By comparing the doped-KCl spectrum with the undoped-KCl spectrum, it is found that the so-called D band is considerably superimposed on the exciton band in both the $KCl:Tl^+$ and $KCl:In^+$ crystals. Unlike the cases of $KI:Sn^{2+}$, $KCl:Sn^{2+}$, and $KI:Tl^+$ the peak of the D band cannot be observed clearly in the absorption spectrum. An absorption band, however, was obtained by subtracting the exciton tail observed in undoped KCl from the absorption spectrum of $KCl:Tl^+$. Indeed Aoyagi and Kuwabara[2] have shown from the excitation spectrum in $KCl:Tl^+$ that the D band is peaking at 7.19 eV.

A considerably weak band is observed at about 6.72 eV in $KCl:Tl^+$ as shown in Fig. 4(a). The 6.72 eV band is so weak that its origin was not established clearly. The band, however, is believed to be due to Tl^+ just as the A, B, and C bands because (1) the similar band has been observed in $KCl:Tl^+$ by Wagner[16] and by Teegarden[17] (see also Fig. 2 of Ref. 13), and (2) the 6.72 eV band appears to grow with Tl^+ concentration.

The similar band is observed at about 6.70 eV in $KCl:In^+$ as seen in Fig. 4(b). The intensity of the 6.70 eV band is 0.30 times of the A band and estimated to be $f=0.0038$ at 77 K. The weak band observed in $KCl:Tl^+$ and $KCl:In^+$ is called D_1 band, whereas the absorption band superimposed on the exciton band is called D_2 band.

From the experimental results, although two components (D_1 and D_2 or D_2 and D_3) have been observed in six crystals of $KCl:Sn^{2+}$, $KI:Tl^+$, $KCl:Tl^+$, $KCl:In^+$, $KI:In^+$, and $KI:Ga^+$, it is generally suggested that the D band is composed of three bands (D_1, D_2, and D_3 in the order of increasing energy; the D_1 is the weakest, the D_2 is the strongest, and the D_3 is observed at a very low temperature) as observed in $KI:Sn^{2+}$. The reason why this remaining D_3 or D_1 component was not observed in the six crystals is believed to be that (1) the measure-

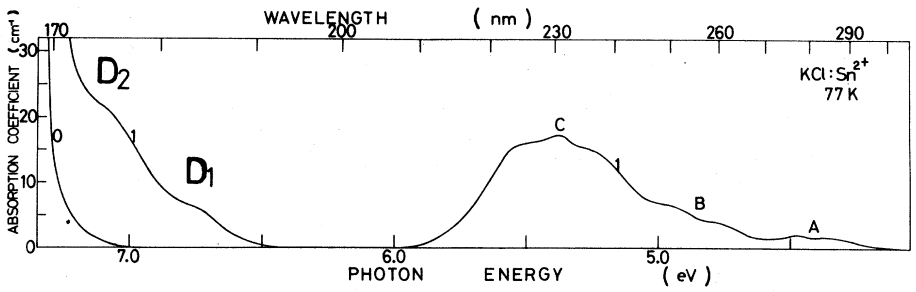

FIG. 2. Absorption spectra of a $KCl:Sn^{2+}$ (0.003 mole % in the melt, curve 1) and an undoped KCl (curve 0) crystals at 77 K.

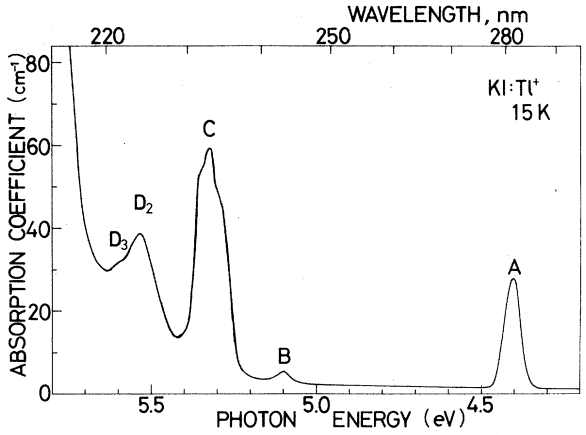

FIG. 3. Absorption spectrum of a KI : Tl⁺ (0.000 34 mole %) crystal at 15 K.

ment was not carried out at low temperatures such as liquid helium temperature, (2) the stronger C and/or exciton bands are located close to the D band, or (3) the remaining component happens to overlap with one of the detected D components.

III. FINE STRUCTURE OF THE THEORETICALLY DERIVED D BAND

In I we made an MO calculation with the extended Hückel method and obtained energies of the a_{1g} and t_{1u} levels including the a_{1g}^* and t_{1u}^* levels responsible for the A, B, and C bands. From the obtained energy level diagram [Fig. 3(a) in I], it was confirmed that the $a_{1g}^* \rightarrow t_{1u}^*$ transition gives rise to the A, B, and C bands, since the lowest allowed transition corresponds to the $a_{1g}^* \rightarrow t_{1u}^*$ transition and the one-electron energy difference W_0 is 5.96 eV in agreement with experiment.

The next allowed transition in the energy level diagram may correspond to the transition from the a_{1g}^* level to a high t_{1u} level of 0.612 eV. The one-electron energy difference in this transition, however, is 9.025 eV which is too high to attribute to the D band in KCl : Tl^+. Zavt and Kristoffel[14] have shown that an e_g-like level, which is constructed mainly by Cl^- $3p$ orbitals around the Tl center, is located at 1.56 eV below the a_{1g}^* level and at 0.44 eV above the valence band [see Fig. 3(e) in I]. The one-electron energy difference W_1 between the e_g and t_{1u}^* levels is estimated as 7.52 eV, which is quite close to the energy of the observed D band. The energies of other allowed transitions, e.g., transitions from t_{1g}, t_{2g}, and a_{1g} levels [see Fig. 3(e) in I] to the t_{1u}^* level, are higher than the exciton-band energy. Thus, it is concluded that only the $e_g \rightarrow t_{1u}^*$ and $a_{1g}^* \rightarrow t_{1u}^*$ transitions give rise to absorption at the low-energy side of the exciton band. Therefore the $e_g \rightarrow t_{1u}^*$ transition [exactly speaking, $(e_g)^4 - (e_g)^3(t_{1u}^*)$ transition] is suggested to be responsible for the D band.

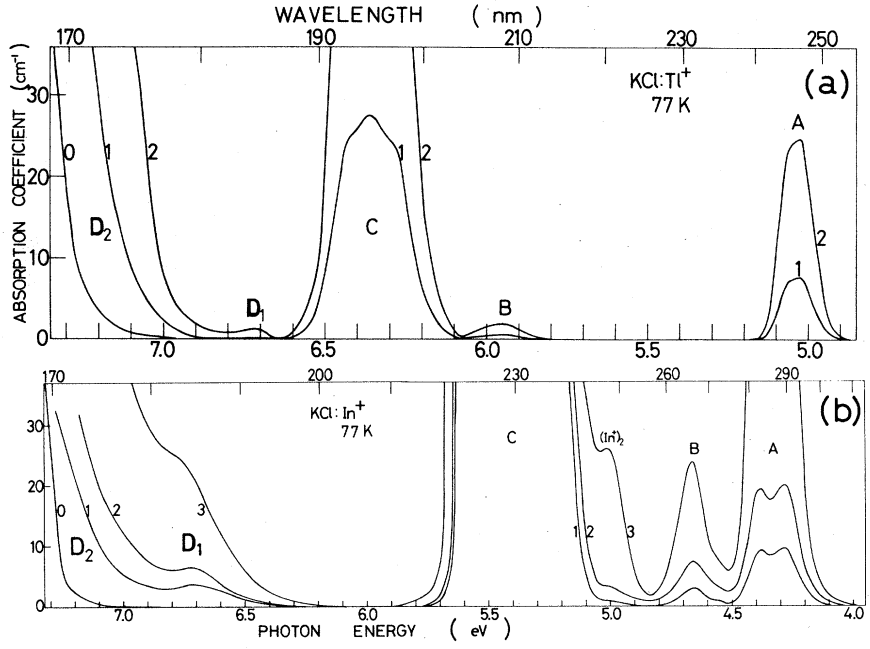

FIG. 4. (a) Absorption spectra at 77 K of an undoped KCl crystal (curve 0) and of KCl : Tl⁺ [0.0003 mole % in the melt (curve 1); 0.001 mole % (curve 2)] crystals. (b) Absorption spectra at 77 K of an undoped KCl crystal (curve 0) and of KCl : In⁺ [0.000 33 mole % (curve 1); 0.000 63 mole % (curve 2); 0.002 mole % (curve 3)] crystals.

TABLE I. Matrix elements between the multiplets T'_{1u} derived from $(e_g)^3$ (t^*_{1u}) and (a^*_{1g}) (t^*_{1u}) configurations. These are quoted from Honma (Ref. 18) except three diagonal elements in the upper block associated with the $(e_g)^3$ (t^*_{1u}) configuration. The three are modified from the Honma's matrix elements and partially expressed with the one electron energy difference.

	$\|3\beta, T'_{1u}\rangle$	ψ_3	$\|3\alpha, T'_{1u}\rangle$	ψ_1	$\|1, T'_{1u}\rangle$
$\|3\beta, T'_{1u}\rangle$	$\frac{1}{2}(F_{ux}-F_{vx})-K_{ux}$ $-K_{vx}-\frac{1}{4}\zeta+W_1$	$-\zeta\sqrt{3/8}$	$-\zeta\sqrt{3}/4$	0	0
ψ_3		$-\frac{1}{2}(F_{ux}-F_{vx})+K_{ux}$ $-K_{vx}+W_1$	$-\zeta/\sqrt{8}$	$2\langle ux\|e^2/r_{12}\|zs\rangle$ $-\langle uz\|e^2/r_{12}\|sz\rangle$	0
$\|3\alpha, T'_{1u}\rangle$			$-\frac{1}{2}(F_{ux}-F_{vx})-K_{ux}$ $-K_{vx}+\frac{1}{4}\zeta+W_1$	0	$-\langle ux\|e^2/r_{12}\|sz\rangle$
ψ_1				$G+W_0$	$\zeta/\sqrt{2}$
$\|1, T'_{1u}\rangle$					$-G-\frac{1}{2}\zeta+W_0$

The ground-state configuration $(e_g)^4$ produces a $^1A_{1g}$ state in an octahedral crystal field, whereas the excited-state configuration $(e_g)^3$ (t^*_{1u}) three states $^1T_{1u}$, $^3T_{1u}$, and $^3T_{2u}$. The transition from the $^1A_{1g}$ state to the $^1T_{1u}$ is dipole-allowed whereas the transitions to the $^3T_{1u}$ and $^3T_{2u}$ states are spin-orbit allowed. Honma has investigated the electronic states of the $(e_g)^3$ (t^*_{1u}) configuration theoretically.[18] He denoted the singlet state $^1T_{1u}$ by $|\psi_3\rangle$ whereas he classified the triplet states in terms of the irreducible representations of the octahedral double group O'_h. Of the triplet states, the state contributing to the allowed transition is represented by $|3\alpha, T'_{1u}\rangle$ for the $^3T_{1u}$ and by $|3\beta, T'_{1u}\rangle$ for the $^3T_{2u}$. In Table I are shown the Hamiltonian matrix elements[18] for the $|\psi_3\rangle$, $|3\alpha, T'_{1u}\rangle$ and $|3\beta, T'_{1u}\rangle$ states of the $(e_g)^3$ (t^*_{1u}) configuration together with the matrix elements for the $^1T_{1u}$ (denoted by $|\psi_1\rangle$) and $^3T_{1u}$ (denoted by $|1, T'_{1u}\rangle$) states of the (a^*_{1g}) (t^*_{1u}) configuration. In the table we have taken into account the configuration interaction between the $(e_g)^3$ (t^*_{1u}) and (a^*_{1g}) (t^*_{1u}).

Among parameters appearing in Table I, the exchange energy G and spin-orbit energy ζ were calculated in I; namely, $G=0.32$ eV and $\zeta=0.46$ eV. The remaining parameters, Coulomb integrals F_{ux} and F_{vx}, and exchange integrals K_{ux} and K_{vx} are defined as follows:

$$\begin{aligned} F_{ux} &= (u^2|e^2/r_{12}|z^2), \\ F_{vx} &= (v^2|e^2/r_{12}|z^2), \\ K_{ux} &= \langle uz|e^2/r_{12}|zu\rangle, \\ K_{vx} &= \langle vz|e^2/r_{12}|zv\rangle, \end{aligned} \tag{1}$$

where round brackets denote Coulomb integrals, e.g., $(u^2|e^2/r_{12}|z^2)$ is the same as $\langle uz|e^2/r_{12}|uz\rangle$. In the matrix elements of Table I appear four orbitals: z, s, u, and v. The z means a z-like MO of the t^*_{1u}, and the s means the a^*_{1g} MO; namely,

$$\begin{aligned} |z\rangle &= c_1(6p_z)+\frac{c_2}{\sqrt{2}\lambda_2}(z_3-z_6)+\frac{c_3}{2\lambda_3}(x_2+y_1-x_4-y_5) \\ &\quad +\frac{c_4}{\sqrt{2}\lambda_4}(s_3-s_6), \\ |s\rangle &= c_1(6s)+\frac{c_2}{\sqrt{6}\lambda_2}\sum_{k=1}^{6}z_k+\frac{c_3}{\sqrt{6}\lambda_3}\sum_{k=1}^{6}s_k, \end{aligned} \tag{2}$$

where the coordinate system, notations of the atomic wave functions, and values of the coefficients c_i and λ_i are described in I. The u and v are basis orbitals of the e_g. They are constructed by the Cl^- $3p$ wave functions z_i:

$$\begin{aligned} u &= \frac{1}{\sqrt{12}\lambda'}(2z_3+2z_6-z_1-z_2-z_4-z_5), \\ v &= \frac{1}{2\lambda'}(z_1+z_4-z_2-z_5), \end{aligned} \tag{3}$$

where the normalization constant λ' is 0.974.

Using the method of intermediate neglecting of differential overlap (INDO),[19] and ignoring two-center Coulomb integrals in which the distance of two centers is more than the next-nearest-neighbor lattice distance, we obtain (in eV)

$$\begin{aligned} F_{ux}-F_{vx} \simeq \tfrac{1}{12}\{&8[c_1(t^*_{1u})]^2[(z_3^2|e^2/r_{12}|6z^2)-(z_1^2|e^2/r_{12}|6z^2)]+4[c_2(t^*_{1u})]^2(z_3^2|e^2/r_{12}|z_3^2) \\ &-2[c_3(t^*_{1u})]^2(z_1^2|e^2/r_{12}|y_1^2)+4[c_4(t^*_{1u})]^2(z_3^2|e^2/r_{12}|s_3^2)\} = 1.18, \end{aligned} \tag{4}$$

$$2K_{uz}\simeq\frac{1}{6\lambda'^2}\left(8[c_1(t_{1u}^*)]^2\langle z_3 6p_z|e^2/r_{12}|6p_z z_3\rangle+4\frac{[c_2(t_{1u}^*)]^2}{\lambda_2^2}(z_3^2|e^2/r_{12}|z_3^2)\right.$$
$$\left.+4\frac{[c_4(t_{1u}^*)]^2}{\lambda_4^2}\langle z_3 s_3|e^2/r_{12}|s_3 z_3\rangle+\frac{[c_3(t_{1u}^*)]^2}{\lambda_3^2}\langle z_1 y_1|e^2/r_{12}|y_1 z_1\rangle\right)=1.01\,, \tag{5}$$

$$K_{vz}\simeq\frac{[c_3(t_{1u}^*)]^2}{4\lambda'^2\lambda_3^2}\langle y_1 z_1|e^2/r_{12}|z_1 y_1\rangle+\frac{[c_1(t_{1u}^*)]^2}{\lambda'^2}\langle 6p_z z_1|e^2/r_{12}|z_1 6p_z\rangle=0.01\,. \tag{6}$$

In the above estimation we used the following values of the one- and two-center integrals:

$$\begin{aligned}&(z_3^2|e^2/r_{12}|6p_z^2)=4.84,\quad (z_1^2|e^2/r_{12}|6p_z^2)=3.89\,,\\&(z_1^2|e^2/r_{12}|y_1^2)=10.57,\quad (z_3^2|e^2/r_{12}|s_3^2)=6.49\,,\\&(z_3^2|e^2/r_{12}|z_3^2)=11.97\,,\ \langle z_3 6p_z|e^2/r_{12}|6p_z z_3\rangle=0.62\,,\ \langle 6p_z z_1|e^2/r_{12}|z_1 6p_z\rangle=0.01\,,\\&\langle z_3 s_3|e^2/r_{12}|s_3 z_3\rangle=0.33,\quad \langle z_1 y_1|e^2/r_{12}|y_1 z_1\rangle=0.70\,,\ \langle 6p_z z_3|e^2/r_{12}|6s z_3\rangle=1.08\,,\end{aligned} \tag{7}$$

which were calculated using the Slater-type atomic orbitals given in I. (Especially, for the two-center integrals, we used Gaussian-type orbitals[20] in order to facilitate the calculation.) The other quantities appeared in the matrix elements are estimated (in eV) as

$$\langle uz|e^2/r_{12}|zs\rangle\simeq\frac{2}{\sqrt{6}}c_1(t_{1u}^*)c_2(t_{1u}^*)c_1(a_{1g}^*)\langle 6p_z z_3|e^2/r_{12}|6s z_3\rangle+\frac{1}{3\sqrt{2}}[c_2(t_{1u}^*)]^2c_2(a_{1g}^*)(z_3^2|e^2/r_{12}|z_3^2)$$
$$+\frac{1}{3\sqrt{2}}c_2(t_{1u}^*)c_4(t_{1u}^*)c_3(a_{1g}^*)(s_3^2|e^2/r_{12}|z_3^2)$$
$$+\frac{1}{3\sqrt{2}}[c_4(t_{1u}^*)]^2c_2(a_{1g}^*)\langle s_3 z_3|e^2/r_{12}|z_3 s_3\rangle=-0.29\,, \tag{8}$$

$$\langle uz|e^2/r_{12}|sz\rangle\simeq\frac{2}{3\sqrt{2}}[c_1(t_{1u}^*)]^2c_2(a_{1g}^*)(6p_z^2|e^2/r_{12}|z_3^2)-\frac{2}{3\sqrt{2}}[c_1(t_{1u}^*)]^2c_2(a_{1g}^*)(z_1^2|e^2/r_{12}|6p_z^2)$$
$$+\frac{1}{3\sqrt{2}}[c_2(t_{1u}^*)]^2c_2(a_{1g}^*)(z_3^2|e^2/r_{12}|z_3^2)-\frac{1}{6\sqrt{2}}[c_3(t_{1u}^*)]^2c_2(a_{1g}^*)(z_1^2|e^2/r_{12}|y_1^2)$$
$$+\frac{1}{3\sqrt{2}}[c_4(t_{1u}^*)]^2c_2(a_{1g}^*)(z_3^2|e^2/r_{12}|s_3^2)$$
$$+\frac{1}{3\sqrt{2}}c_2(t_{1u}^*)c_4(t_{1u}^*)c_3(a_{1g}^*)\langle z_3 s_3|e^2/r_{12}|s_3 z_3\rangle=-0.58\,. \tag{9}$$

Here, the values of non-overlap coefficients c_i's appearing in Table I of I were used in Eqs. (4), (8), and (9). Using the above values, we diagonalize the 5×5 matrix of Table I. The eigenvalues and eigenvectors obtained are shown in Table II, where the eigenstates are denoted by A, C, D_1, D_2, and D_3. [The A and C states consist mainly of $^3T_{1u}$ and $^1T_{1u}$ components associated with the $(a_{1g}^*)(t_{1u}^*)$ configuration, respectively, and the D_1, D_2, and D_3 states consists mainly of $^3T_{1u}$, $^1T_{1u}$, and $^3T_{2u}$ components associated with the $(e_g)^3$ (t_{1u}^*), respectively.]

Next we calculate the momentum matrix elements $\langle\psi_1,x|\sum_i\hat{p}_i^x|\mathcal{G}\rangle$ and $\langle\psi_3,x|\sum_i\hat{p}_i^x|\mathcal{G}\rangle$ to try to estimate the transition intensity, where $\hat{p}_i^x$ is an x component

TABLE II. Calculated eigenvectors, energies E, and squares of matrix elements $|P|^2$ (in units of 10^{-2} a.u.) of the A, C, D_1, D_2, and D_3 states. Experimental data of energy E and oscillator strength f for the A, C, D_1, D_2, and D_3 bands are also shown.

	Theory							Experiment	
	$\|3\beta,T_{1u}'\rangle$	$\|\psi_3\rangle$	$\|3\alpha,T_{1u}'\rangle$	$\|\psi_1\rangle$	$\|1,T_{1u}'\rangle$	E (eV)	$\|P\|^2$	E (eV)	f
D_3	0.752	−0.658	−0.040	−0.002	−0.010	7.74	2.37		
D_2	0.581	0.692	−0.405	−0.043	−0.133	7.28	3.10	7.23[b]	~0.22
D_1	0.298	0.287	0.748	0.313	0.413	6.71	0.09	~6.72	
C	−0.082	−0.075	−0.373	0.917	0.091	6.31	9.28	6.36	0.508[a]
A	−0.034	−0.029	−0.367	−0.244	0.896	5.08	0.48	5.03	0.0804[a]

[a] Obtained from Wagner (Ref. 16).
[b] See *Note added in proof*.

of momentum operator for the ith electron. $|\psi_1, x\rangle$ is the x-like basis of the $|\psi_1\rangle$ state, and $|\mathcal{G}\rangle$ the ground state, $(e_g)^4(a_{1g}^*)^2$. In I we obtained (in a.u.)

$$\left\langle \psi_1, x \left| \sum_i \hat{p}_i^x \right| \mathcal{G} \right\rangle = i0.313 .$$

On the other hand, $|\psi_3, x\rangle$ state is given as follows:

$$|\psi_3, x\rangle = -\frac{1}{\sqrt{8}} \|u\beta; x\beta\| - \frac{1}{\sqrt{8}} \|u\alpha; x\alpha\| + \sqrt{\tfrac{3}{8}} \|v\beta; x\beta\| + \sqrt{\tfrac{3}{8}} \|v\alpha; x\alpha\| . \quad (10)$$

Here $\|u\beta; x\beta\|$ is the Slater determinant which has $|x\beta\rangle$ orbital of t_{1u}^* in place of $|u\beta\rangle$ orbital of e_g appearing in the closed-shell-type determinant representing the ground state $|\mathcal{G}\rangle$, and α and β indicate up and down spin states, respectively. The momentum matrix element regarding the $|\psi_3, x\rangle$ state (in a.u.) becomes

$$\begin{aligned} \left\langle \psi_3, x \left| \sum_i \hat{p}_i^x \right| \mathcal{G} \right\rangle &= -\frac{2}{\sqrt{8}} \langle x|\hat{p}^x|u\rangle + 2\sqrt{\tfrac{3}{8}} \langle x|\hat{p}^x|v\rangle \\ &\simeq \frac{4}{\sqrt{6}\lambda'} c_1(t_{1u}^*)\langle 6p_x|\hat{p}^x|z_1\rangle \\ &\quad + \frac{2}{\sqrt{3}\lambda'\lambda_4} c_4(t_{1u}^*)\langle s_1|\hat{p}^x|z_1\rangle \\ &= -i0.235 , \end{aligned} \quad (11)$$

where the two-center matrix element $\langle 6p_x|\hat{p}^x|z_1\rangle = -i0.092$ a.u. and the intra-atomic matrix element $\langle s_1|\hat{p}^x|z_1\rangle = -i0.186$ a.u. were used. Using the above values, we can easily evaluate transition intensities for the transitions from the ground state to the A, C, D_1, D_2, and D_3 eigenstates. The square of the momentum matrix element $|P|^2$ is shown in Table II.

IV. DISCUSSION

In Sec. III, we assumed the $(e_g)^4 \rightarrow (e_g)^3 (t_{1u}^*)$ transition as the origin of the D band in KCl : Tl^+, and we made a calculation on this transition taking into account the $(a_{1g}^*)^2 \rightarrow (a_{1g}^*)(t_{1u}^*)$ transition. It is found from Table II that the theoretically derived energies of the A, C, D_1, and D_2 states in KCl : Tl^+ are in good agreement with the experimentally observed positions of the A, C, D_1, and D_2 bands, respectively. It should be noted that the agreement on the A and C bands is more satisfactory than the case of the previous calculation made in I (see Table III in I) in which only the $(a_{1g}^*)(t_{1u}^*)$ configuration was taken into account to understand the A, B, and C bands. As for the D_3 state, the corresponding absorption band (D_3 band) has not been observed experimentally. This is presumably due to the fact that the exciton band peaking at 7.76 eV (Ref. 21) is close to the energy of the D_3 state (i.e., 7.74 eV). Therefore the D_3 band is believed to be hidden by the much stronger exciton band.[22]

The $|P|^2$ ratio of the C band to the D_2 band is theoretically estimated to be 2.99 from Table II. This value is close to the experimental value of about 2.31, which was calculated as the ratio of oscillator strengths of the observed C and D_2 bands. The $|P|^2$ value of the theoretically derived D_1 band is much smaller than those of other bands, suggesting that the D_1 band is too weak to be observed in a very lightly doped crystal. This is consistent with the experimental result. (The theoretical reason for the weak intensity of the D_1 band is that, although each weight of the $|\psi_1\rangle$ and $|\psi_3\rangle$ components in the D_1 state is considerably large as shown in Table II, they cancel each other in the contribution to the momentum matrix element.) From the quantitative comparison between the theoretical and experimental results, it is concluded that the theoretically derived A, C, D_1, and D_2 bands in KCl : Tl^+ agree with the experimentally observed A, C, D_1, and D_2 bands, respectively. We, however, have to point out the following two points with regard to the present calculation.

The one point is the intensity ratio of the C band to the A band. The calculated ratio becomes 19.2, whereas the experimental ratio is 6.3. This discrepancy is due to the smallness of the calculated spin-orbit energy ζ, which was already noticed in I. Another is the justification of the t_{1u}^* level. (In the present calculation, the t_{1u}^* wave function responsible for the A, B, and C bands was used for the D band.) The t_{1u}^* orbital is Tl^+ $6p$-like, whereas the e_g orbital is completely localized at the Cl^- sites. Owing to such a character of the t_{1u}^* and e_g orbitals, the transition $e_g \rightarrow t_{1u}^*$ appears to stand on the charge-transfer model. Therefore, to obtain more exact results, we have to take into account a change of charge distribution after the ejection of electron from the e_g orbital into the t_{1u}^* orbital and calculate self-consistently the final state t_{1u}^* in a redefined potential. The new t_{1u}^* state is possibly a little diffuse, and, strictly speaking, the quantities appearing in Table I should be re-examined. However, about a half of the original t_{1u}^* orbital, which is responsible for the A, B, and C bands, consists of the Cl^- $3p$ and $4s$ wave functions (see I); that is, the t_{1u}^* orbital extends into the ligand Cl^- ions considerably. Therefore, we believe that the present calculation is not so unreasonable.

As mentioned above, it has been clarified that the D band in KCl : Tl^+ is composed of three bands, D_1, D_2, and D_3, and that the weakest D_1 band is located at the lowest energy, the D_2 band is the

strongest, and the relatively strong D_3 band is located close to the exciton band. The characteristics of the D band are similar to the case of the D band observed in KI : Sn^{2+} (see Fig. 1) and are partially similar to the cases of other alkali halides doped with s^2 ions. Therefore, although the detailed MO calculation has not been made, it is suggested that the $(e_g)^4 \rightarrow (e_g)^3 (t_{1u}^*)$ transition gives rise to the D band in not only KCl : Tl^+ but in other alkali halides. In the following paragraph we qualitatively show that the assignment of the D band to such a charge-transfer transition is certainly applicable to the other s^2-ion-doped alkali halides.

As shown in Figs. 1–4, the D-band position of Tl^+-doped potassium halides moves to lower energy in going from KCl to KI, and the same is true for the D band of Sn^{2+}-doped potassium halides. This agrees with our idea that the D band is attributable to ligand → metal charge-transfer transition, since charge-transfer spectra, in general, move to lower energies when halogen ligands are varied from F^- to Cl^- to Br^- and to I^- around a definite central (metal) ion because of the decrease of optical electronegativity in going from F^- to Cl^- to Br^- to I^-.[23] Moreover, it is observed in Figs. 1–4 that the D-band energy decreases in KI crystals as the metal ion is varied from Tl^+ to Sn^{2+}. The same is true for KCl crystals. This decrease is expected for the charge-transfer band because of the increasing ionization energy of metal ion. It is noted that the D-band energy is almost the same between KCl : In^+ and KCl : Tl^+ as seen in Fig. 4. This is consistent with the above idea because the ionization energy of In is almost the same as that of Tl when compared with that of Sn. Like this, the transition energy of the D band varies with not only the ionization energy or oxidation state of metal ion but the optical electronegativity of halide ion, suggesting that the D band arises from the halide → metal charge-transfer transition. Our present MO calculation is based on the extended Hückel method in which the ionization potential and oxidation state of metal and halide ions are also taken into account. Therefore, although the similar MO calculation (including the configuration interaction) has not been carried out for KCl : In^+, KCl : Sn^{2+}, KI : Tl^+, and KI : Sn^{2+}, we believe that the experimental data of Figs. 1–4 may be quantitatively explained using the charge-transfer model as the case of KCl : Tl^+.

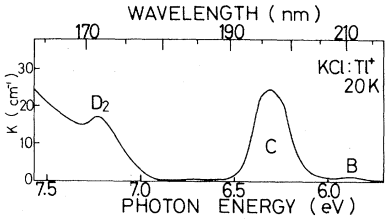

FIG. 5. Absorption spectrum of KCl : Tl^+ (crystal thickness is 0.49 mm) at 20 K. K: absorption coefficient.

Note added in proof. While this manuscript was in press we tried to find the peak of the D band in KCl : Tl^+. By the measurement of very lightly doped crystal at 20 K, the peak of D_2 band was clearly observed at 7.23 eV as shown in Fig. 5.

[1]P. H. Yuster and C. J. Delbecq, J. Chem. Phys. 21, 892 (1953).
[2]K. Aoyagi and G. Kuwabara, J. Phys. Soc. Jpn. 15, 2334 (1960).
[3]A. Fukuda, Sci. Light (Tokyo) 13, 64 (1964).
[4]K. Inohara, Sci. Light (Tokyo) 14, 92 (1965).
[5]T. Mabuchi, A. Fukuda, and R. Onaka, Sci. Light (Tokyo) 15, 79 (1966).
[6]Ch. Lushchik, R. Gindina, S. Zazubovich, and N. Lushchik, Czech. J. Phys. B 20, 585 (1970).
[7]T. Kamejima, A. Fukuda, and S. Shionoya, J. Phys. Soc. Jpn. 30, 1124 (1971).
[8]T. Tsuboi, Y. Nakai, K. Oyama, and P. W. M. Jacobs, Phys. Rev. B 8, 1698 (1973).
[9]U. Mayer, D. Schmid, and H. Seidel, Phys. Status Solidi B 70, 269 (1975).
[10]T. Tsuboi, Phys. Status Solidi B 96, 321 (1979).
[11]T. Tsuboi, Physica B 96, 341 (1979).
[12]T. Tsuboi, M. J. Stillman, and P. W. M. Jacobs, Chem. Phys. Lett. (in press).
[13]R. S. Knox, Phys. Rev. 115, 1095 (1959).
[14]G. S. Zavt and N. N. Kristoffel, Ukr. J. Phys. 19, 203 (1974); N. N. Kristoffel, G. S. Zavt, and B. V. Schulichenko, in *Physics of Impurity Centres in Crystals*, edited by G. S. Zavt (Academy of Sciences of the Estonian SSR, Tallin, USSR, 1972), p. 53.
[15]S. Sakoda and T. Tsuboi, preceding paper, Phys. Rev. B 22, 4966 (1980).
[16]W. U. Wagner, Z. Phys. 181, 143 (1964).
[17]K. Teegarden, in *Luminescence of Inorganic Solids*, edited by P. Goldberg (Academic, New York, 1966), p. 84.
[18]A. Honma, Sci. Light (Tokyo) 22, 101 (1973); 23, 1 (1974).
[19]J. A. Pople and D. L. Beveridge, in *Approximate Molecular Orbital Theory* (McGraw-Hill, New York, 1970), Chap. 3.
[20]H. Taketa, S. Huzinaga, and K. O-ohata, J. Phys. Soc. Jpn. 21, 2313 (1966).
[21]J. E. Eby, K. J. Teegarden, and D. B. Dutton, Phys. Rev. 116, 1099 (1959).
[22]The result of the present calculation explains why the

peak of the D_2 band has not been observed in the absorption spectrum 77 K. For, the theoretically derived D_2 band is located at 7.28 eV, whereas the stronger absorption due to exciton starts from about 7.3 eV (see Fig. 4), indicating that the D_2 band is considerably superimposed on the exciton-band tail.

[23] An excellent review on the charge-transfer band has been given by Professor D. S. McClure and Professor C. K. Jørgensen: D. S. McClure, in *Treatise on Solid State Chemistry*, edited by N. B. Hannay (Plenum, New York, 1975), Vol. 2, Chap. 1; J. Lumin. 12/13, 67 (1976); C. K. Jørgensen, in *Modern Aspects of Ligand Field Theory* (North-Holland, Amsterdam, 1971).